Available online at www.sciencedirect.com

ScienceDirect

Energy Procedia 35 (2013) 285 – 296

Energy Procedia

DeepWind'2013, 24-25 January, Trondheim, Norway

Experimental investigation of wind turbine wakes in the wind tunnel

Heiner Schümann[a]*, Fabio Pierella[a], Lars Sætran[a]

[a] *Norwegian University of Science and Technology, N-7491, Trondheim, Norway*

Abstract

Detailed wake measurements with two similar model wind turbines, with a diameter of 0.9m, were performed in the wind tunnel. A single turbine arrangement and a tandem setup, where a wind turbine was operated in the wake of an upstream wind turbine, were tested. Measurements of the cross section in the near and far wake as well as measurements in axial direction are presented. A single hot-wire and a five-hole probe were used. The application of the five-hole probe enabled to measure a three-dimensional flow field providing detailed inspections of the rotation of the wake. A strong tower wake and a non-uniform velocity field and turbulence distribution were observed.

Keywords: Wind turbine wake, Wake interaction, Wake rotation, Tower wake,Turbulence intensity, Velocity field

1. Introduction

Wind turbines operating in the wake of an upstream turbine are exposed to conditions which are significantly different from a free standing turbine. The incoming flow field is characterized by a non-uniform velocity profile and turbulence intensities significantly higher than in the free stream. The velocity deficit reduces the available energy in the wind and hence, the power produced by the downstream turbines. High turbulence intensities induce strong variable forces on the blades and can significantly increase the fatigue. In wind farms a separating distance of six to ten rotor diameters in the predominant wind direction is common and even if the velocity deficit has mainly recovered at this distance the turbulence effects might still be noticeable at 15 rotor diameters downstream of a turbine. [1]

For a further improvement of wind turbines and wind farms a better understanding of wake

* Corresponding author. Tel.: +47-94244119
E-mail address: heiner.schumann@ntnu.no.

doi:10.1016/j.egypro.2013.07.181

aerodynamics is necessary. Many details are still not understood and worldwide energy research shows a shift towards more fundamental 'Back to Basics' approach, which means experiments under controlled conditions [2]. Detailed wake measurements, especially full cross-sectional measurements, are rare [3]. Even if time consuming, such experiments are absolutely necessary for a better understanding of wake aerodynamics and to provide a solid benchmark for wind turbine wake models.

A review of wind turbine aerodynamics is given by Sanderse [1]. A rotating wake surrounded by a highly turbulent shear layer as transition zone to the undisturbed fluid is reported. The lowest velocity in the wake is reached around one to two diameters downstream of the rotor [4] and the end of the near wake region is mentioned to be between two and five diameters, when the expanding shear layer reaches the center [1], [2]. As mixing of the turbulent and undisturbed fluid takes place, the wake expands. Experiments where an atmospheric shear layer was simulated [5] showed that the maximum velocity deficit point had a tendency to shift below the rotor axis and led to a non-symmetric distribution of atmospheric turbulence with respect to the rotor axis, with lower turbulence level registered closer to the ground. However, no shear in the mean flow was present during wind tunnel experiments presented in this paper.

An overview over wind turbine experiments and computations with emphasis placed on near wake aerodynamics is given by Vermeer et al. [2].

In this paper high resolution near and far wake measurements of a single turbine setup and a tandem setup, where a wind turbine was operated in the wake of an upstream turbine, are presented. The work is a continuation of a previous measurement campaign performed by Bartl et al. [6] on the same model wind turbines, positioned three and five rotor diameters apart. Bartl et al. inspected the influence of the separation distance on the performance of the downstream turbine in addition to wake measurements behind the two machines. However, only the axial velocity component was measured. Extensive studies of the tower influence were conducted by Nygard [7] and Blomhoff [8] using the same model wind turbines. Nygard found that a deflection of the tower wake occurred which depended on the operational condition. Blomhoff operated a single turbine setup with a to the real tower identical fake tower mounted on top of the wind turbine. Restoring the geometric symmetry also restored the symmetry of the rotating wake, which proved the influence of the tower on asymmetries in the rotor wake.

Similar experiments, including wake and performance measurements of an array of two model turbines, were performed by Maeda et al. [3]. The results showed that the downstream turbine efficiency was significantly lower than the upstream one. Axial velocity measurements downstream a single turbine showed a complex wake structure, highly non-axisymmetric, where the maximum velocity deficit did not lie on the rotor axis (Figure 8, page 204). Smith [9] presented velocity, turbulence and shear stress measurements of the wake behind a single model wind turbine and two in-line setups of two turbines with a separation distance of five and seven and a half diameters, respectively. An interesting result is that the maximum velocity deficit behind an array of two wind turbines recovers faster than behind a single machine (3 Summary of the experimental results, page 326). An extensive wind tunnel study of the up and downstream flow field as well as performance measurements were presented by Medici [10]. Measurements with different model turbines with a rotor diameter around 0.2m using Particle Image Velocimetry (PIV) and Hot-wire anemometry were conducted in a closed-loop wind tunnel.

Adaramola and Krogstad [11] studied the effect of the separation distance, blade pitch angle and yaw angle on the total power output of an in-line setup of two model turbines. The highest total power output was reached by operating the upstream turbine slightly outside its optimum. Near wake and performance measurements of a yawed turbine at varying TSR were investigated by Krogstad and Adaramola [12]. Krogstad and Eriksen [13] presented results from the "Blind test" workshop. Eight groups of researchers tried to predict wind tunnel data of the single turbine, also applied in the current work, by different numerical methods. A comparison showed good agreement of the power generation and thrust force while the predicted wake velocity defect and turbulent kinetic energy was more uncertain. Recently a second

blind test was carried out. This time an in-line setup of two model wind turbines, very similar to the present work, was used as the test case [14].

Nomenclature

D	diameter of the rotor (0.9m)
r	radial distance from the rotational axis
R	radius of the rotor (0.45m)
TSR	tip speed ratio
u'	standard deviation of the local velocity measurements
U_m	time-averaged velocity
U_∞	free stream velocity
u'/U_m	turbulence intensity with U_m = local mean velocity
V_{transv}	transversal velocity (velocity in the plane)
x, y, z	distance from the origin in the respective direction in the Cartesian coordinate system
γ	swirl angle
U_x	velocity component in x-direction
U_{tan}	tangential velocity component

2. Experimental Setup

2.1 Measurement apparatus

The measurements were performed in the large closed loop wind tunnel of the Department of Energy and Process Engineering at The Norwegian University of Science and Technology. The wind tunnel had a closed test section with the dimensions of 1.9m (height) x 2.7m (width) x 11m (length). Two three-bladed model wind turbines with approximately equal dimensions of 0.9 m rotor diameter and a hub height of 1m were available and could be placed freely in the wind tunnel. The turbines were equipped with identical blades. For details the reader is referred to Krogstad, et al. [15]. Each turbine axis was coupled to an electric AC motor with a maximum power output of 0.37kW by belt transmission. The motor was controlled via a Siemens Micromaster 440 frequency inverter which, in combination with an optical rpm sensor, provided the ability to finely adjust the rotational speed. The motor was either driving the turbine or working as generator when the turbine was extracting energy from the wind. The torque could be measured via torque sensors mounted to the turbine shafts.

The velocity distribution in the wake behind the turbines was measured by a five-hole probe, calibrated by a routine described by Morrisson et al. [16]. Accurate measurements of flow angles up to 20° were possible. For larger angles up to 40° the probe still gave satisfactory results but resulting in uncertainties larger than 10%. The turbulence intensity was measured by a single hot-wire probe (CTA – constant temperature anemometry). Both probes were mounted to a four-axis traverse system attached to the roof

of the wind tunnel. The traverse was controlled by a LabVIEW program. For the hot-wire probe the sampling rate and sampling time were 8000 samples/s and 40s respectively. For the five-hole probe the sampling rate and sampling time were 30 samples/s and 15s respectively. Hence, all results are presented as time averaged values. A present LabVIEW program was extended towards fully automatic measurements. A beforehand generated measurement grid could automatically be traversed. The separation distance of the grid points was 6cm. In the outer region of the grid a lower resolution was chosen and the separation distance between the measurement points was increased to 8 to 12cm. A measurement grid for one cross section, 1.7 x 1.8m, consisted of over 500 measurement points. The measured parameters and the exact position were recorded and could subsequently be easily analyzed.

2.2 Arrangements

Measurements with two different setups were performed. For the first arrangement a single turbine was placed in the wind tunnel. The rotor of the model turbine was placed four rotor diameters downstream of the test section inlet. The velocity distribution in a plane perpendicular to the rotor axis at the positions x/D = 0.6D and x/D = 3D downstream of the rotor plane was measured by a five-hole probe. Fig. 1 (top) shows the single turbine arrangement with the measurement positions.

In the second setup, a second turbine with an identical blade set was placed three rotor diameters upstream of the first turbine. Again the velocity distribution was measured by a five-hole probe. In addition, the stream wise turbulence intensity u'/U_m, where u' = standard deviation of the local velocity and U_m = local mean velocity, was contextually measured with a single hot-wire probe. The probe was traversed in a plane perpendicular to the rotor axis at the positions x/D = 0.6D and x/D = 3D downstream of the second wind turbine. Furthermore, the upper and the left wake were measured in the x-y plane and the x-z plane respectively, as shown in Fig. 1 (bottom).

During the measurements the free stream velocity was regulated to a constant value of U_∞ = 10.5m/s. The turbines were adjusted to and operated at their optimal operating point, respectively. For the free standing turbine and for the upstream turbine of the tandem arrangement this corresponded to a tip speed ratio of TSR = 6. Thus, the Reynolds number based on the tip speed and the chord length was approximately Re = 1.2 * 10^5. The tip speed of the downstream turbine of the tandem setup was adjusted to its optimal operating point by measuring the torque and hence the power produced. The downstream turbine had a peak in the performance curve at TSR = 4, when the free stream velocity was used as reference.

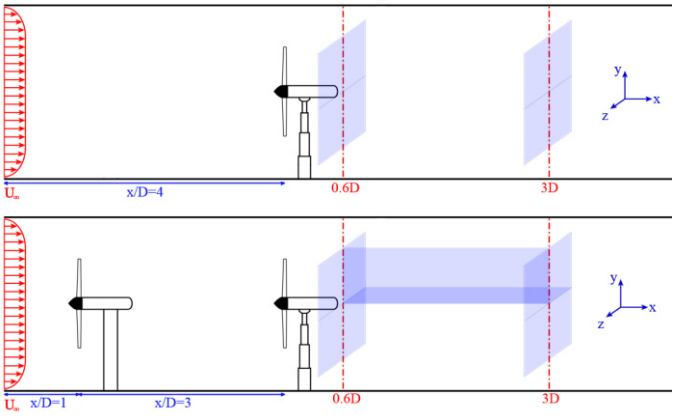

Fig. 1: Single turbine setup (top), tandem setup (bottom).

2.3 Uncertainty and blockage effects

The measurement instruments were extensively calibrated before every measurement campaign (the hot-wire probe also after each experiment) and the uncertainties of the velocity measurements were calculated to be less than 10 %. Random comparison with velocity measurements by the hot-wire probe resulted in good agreement. However, with respect to directional measurements with larger flow angles where the accuracy is worse 10% is given as an estimate for the upper limit. The equipment was carefully installed. Laser levels and rulers were used to align and position the turbines. Vibrations of the tower during operation and resulting uncertainties of the separation distance were observed to be very low. Therefore, an upper estimate of the uncertainty of the separation distance is 1cm and 1° for the yaw angle (adjusted to be zero). When the blades were mounted a positioning device was used. However, an upper uncertainty estimate of 0.5° is given for the pitch angel. The blades were CNC produced and expected to be very identical and well matching the NREL S-826 profile design. Nevertheless, at low Reynolds numbers of the order of 10^5 small uncertainties can change the characteristics significantly. Sarmast [17] presented experimental 2D data for the the NREL S-826 airfoil at low Reynolds numbers obtained in the DTU wind tunnel.

The blockage ratio of the model turbines, defined as the rotor swept area divided by the wind tunnel cross-sectional area, was 13.5 % and 12.1 % for turbine 1 and turbine 2 respectively. A suggested upper limit in order to avoid wind tunnel wall interference was 10 % [18] which was close to the blockage ratios achieved so the blockage effect was neglected. However, a blockage effect by the wind tunnel walls and the traverse constraining the expansion of the wake further downstream of the turbines was observed. The same blockage effect was achieved by Adaramola et al. [11]. Unfortunately this is difficult to correct for.

3. Results and Discussion

The following results were corrected for temperature and atmospheric pressure changes and normalized by division by the contraction velocity measured at the inlet nozzle and representing the free stream velocity. White areas in the velocity plots belong to flow directions the five-hole probe was not calibrated for and therefore could not be measured.

3.1 Single Turbine

At the distance x/D = 0.6 downstream of the single turbine a relatively symmetric wake extending from z/R = -1.15 to z/R = 1.15 in horizontal direction was measured, as shown in Fig. 2 (left). The blade sweep area showed a relative uniform velocity distribution of $U_m / U_\infty \approx 0.5$. The wake was bordered by a sharp transition zone distinguishable by a thin annular area with steep velocity gradient, the shear region. Velocities in the centre of the wake were slightly higher since no energy extraction from the wind took place in this region. The wake by the tower was visible in the form of a sharp velocity deficit area superimposed to the rotor wake. The arrows, depicting the transversal velocity, show the rotation of the wake in opposite direction to the rotor. The interaction of the rotating fluid of the rotor wake with the tower explains the deflection of the tower shadow observed inside the rotor wake area.

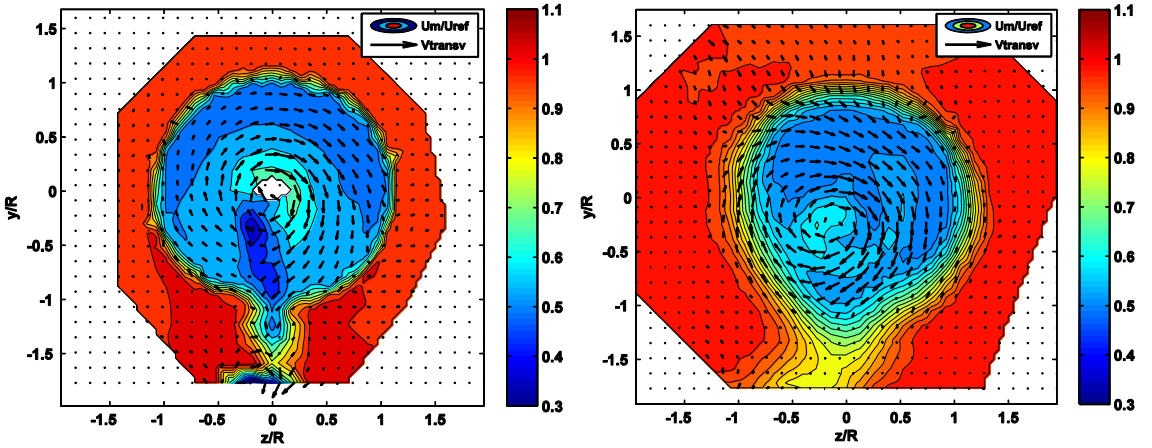

Fig. 2: Normalized velocity U_m/U_∞ as a colour chart, arrows show the transversal velocity intensity and direction, measured at x/D=0.6 (left) and x/D=3 (right) downstream of the single turbine.

With increasing downstream distance from the rotor wake theory predicts an expansion of the wake. This can clearly be seen from the measurements performed at the distance x/D = 3 downstream of the single turbine, as shown by Fig. 2 (right). The horizontal wake extension now reached from z/R = -1.3 to z/R = 1.4. The transition zone had clearly widened and the inner wake showed lower velocity gradients. The velocity deficit created by the tower inside the rotor wake was not clearly distinguishable. The overall shape of the wake was not symmetric anymore. At the bottom the tower wake had merged with the rotor wake. When comparing with cross-sectional measurements taken at x/D = 4 downstream of a single turbine by Maeda et al. [3] (Figure 8, page 204) many similarities can be spotted: the deformation of the tower wake and especially the overall shape of the wake are in good agreement with the current results.

3.2 Tandem Arrangement

The overall shape of the wake downstream of the tandem setup (Fig. 3) had some similarities with the single turbine arrangement, but due to further extraction of energy at x/D = 0.6 downstream of the second turbine the velocity deficit was significantly higher than behind the single turbine. In the inner part of the rotor wake, a relatively uniform velocity distribution of around $U_m / U_\infty \approx 0.35$ was measured. Due to the superposition of the single wakes, the velocity deficit area was broader and had a smoother and wider transition zone than the single wake. An increased wake width and a higher velocity deficit agreed with measurements by Smith [9] (page 330-331). Smith states that the velocity deficit behind the second turbine is less than it would be when predicted by linear superposition and rather depends on the separation distance of the turbines. The tower wake was observable but was, especially inside the rotor wake, less distinct than for a single turbine. As described by Nygard [7] this effect is probably caused by a smaller Reynolds number based on the tower diameter, due to a decrease of incoming air velocity. A similar behaviour was found by Bartl et al. [6]. The tower wake recovers faster also because of the enhanced mixing due to higher turbulence produced by the upstream turbine. This bears analogy to measurements behind a single turbine by Maeda et al. [3] who found a less distinct tower shadow in the wake when the incoming wind field was fully turbulent compared to a smooth one (4.2 “Wake of independent turbine” and Figure 8, page 202-204).

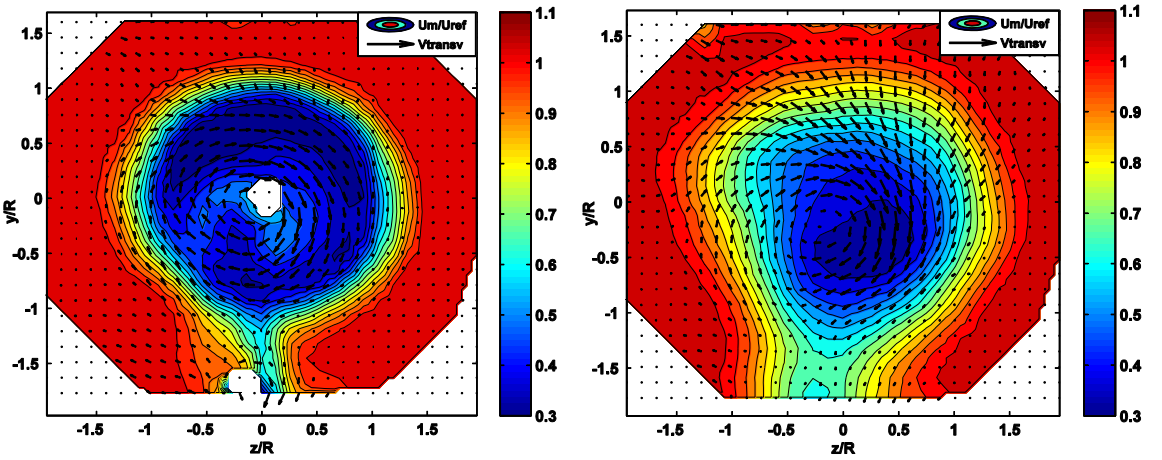

Fig. 3: Normalized velocity U_m/U_∞ as a colour chart, arrows show the transversal velocity intensity and direction, measured at x/D=0.6 (left) and x/D=3 (right) downstream of the tandem setup.

At the distance x/D = 3 downstream of the second turbine, as shown in Fig. 3 (right), the velocity measurements showed an extension of the wake of z/R = ±1.7 in horizontal direction which had increased from z/R = ±1.5 measured at x/D = 0.6. The transition zone had further widened and the wake was further deformed. The tower shadow inside the rotor wake was not observable anymore. The transversal velocity component, represented by the black arrows, tends towards the ground. The same effect was reported by Medici [10], who mentioned that the presence of the ground "bounds and pulls down the wake … further downstream" (page 126).

The highest turbulence intensity was measured in the blade tip region, the centre region and especially behind the tower. It should be mentioned that the hot-wire probe does not distinguish between random turbulence, created by for instance the tower, and vortices as ordered structures, as for example the blade tip vortices. At x/D = 0.6 downstream of the second turbine turbulence intensities greater than 25% were measured, as shown by Fig. 4 (left). The high turbulence in the tip region can partially be ascribed to tip vortices. Vortices shed by the blade roots, in addition to turbulence created by the nacelle, explain the

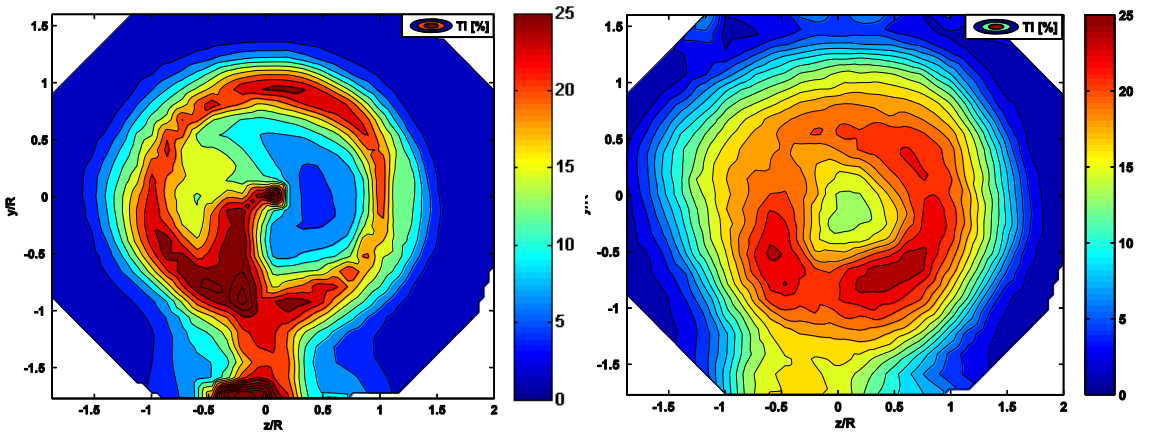

Fig. 4: Turbulence intensity u'/U_m [%] measured at x/D=0.6 (left) and x/D=3 (right) downstream of the tandem setup.

high turbulence values in the centre of the wake. An even higher turbulence intensity of up to 37% was measured behind a tandem setup by Smith [9]. One can clearly observe that the turbulent fluid produced by the tower was deflected in rotational direction.

Further downstream at x/D = 3 the highest turbulence was annularly distributed around the centre of the rotor wake, as shown by Fig. 4 (right). Two local maxima were observed. However, no explicit attribution of tower induced turbulence was possible.

In Fig. 4 the ambient turbulence intensity seems to be zero which is due to the limited number of colour levels chosen to define the contour levels. In fact, even if very low for the present wind tunnel, the real turbulence intensity in the ambient flow is never zero. Traversing the empty wind tunnel in the inlet section and x/D=2 downstream of the inlet section resulted in an average turbulence intensity of 0.5% with all measurements (except of a single measurement close to the bottom plate) below 1%.

A comparison of the velocity measurements in the near and far wake of the single and tandem case (Fig. 2 and Fig. 3) showed a faster recovery of the velocity deficit in the wake of the tandem setup. Additional turbulence is produced by the downstream turbine as found by for instance Bartl et al. [6] or Smith [9] operating a similar setup. The higher turbulence level leads to higher turbulent diffusion and mixing rates which in turn increase the recovery rate. Consequently, the power production decrease between the second and an imaginary third turbine at x/D=3 downstream of the second turbine would be much smaller than the decrease in power production between the first and the second turbine. In wind farms an equilibrium velocity and turbulence value is reached after a certain amount of rows [1]. Smith [9] mentions a further mechanism leading to an increased recovery of velocity deficit based on the shear stress profile. A shear stress profile develops behind the first turbine but is already established for the following turbine which supports turbulent mixing.

3.3 Wake expansion and recovery

Fig. 5 shows velocity and turbulence measurements for the left part of the wake in the x-z plane (at hub height) seen from top. The expansion of the wake as well as the expansion of the transition zone with increasing downstream distance from the rotor was observed. Close to the rotor the highest velocity deficit was found in the outer blade region. Further downstream this region moves towards the centre of the wake. A general velocity component towards the centre (radial velocity) was observed which is in agreement with measurements by Medici [10]. However, in the very near wake Medici found a radial velocity component from the centre to the free stream which reverses towards the centre at around x/D = 1. Even if not observed in our measurements this effect could have been present in a region not measured very close to the rotor.

Fig. 6 (left) shows the expansion of the wake in z-direction. The expansion was defined as the distance where a velocity of $U/U_\infty = 1.04$ is reached which corresponds to the outer contour line of Fig. 5 (left). An acceleration effect of the surrounding fluid due to the blockade of the wind turbine explains why this

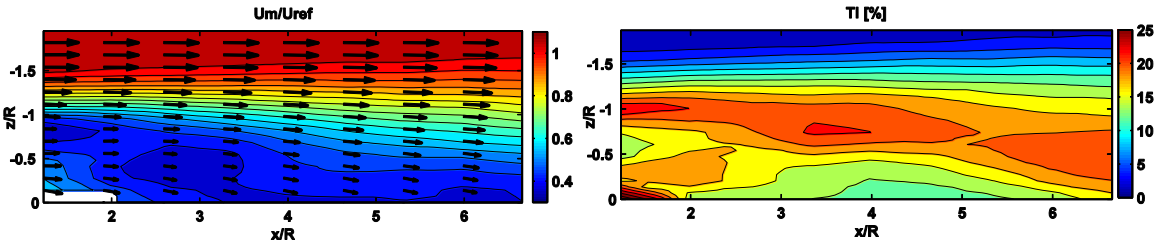

Fig. 5: Normalized velocity U_m/U_∞ (left) and turbulence intensity u'/U_m [%] (right) as a colour, arrows show the transversal velocity intensity and direction, measured in the x-z plane downstream of the tandem setup.

value is higher than unity. At x/R = 0 the expansion width of the single turbine wake at x/R = 6 or x/D = 3 was added representing the starting condition for the second wake. This assumption is not completely true because upstream effects influence the flow and hence the wake of the first turbine. Anyway a faster wake expansion rate close to the rotor was measured. Error bars based on the 10% uncertainty estimate show a wide range. Because of the smaller velocity gradient in radial direction the uncertainty range is increasing for the wake expansion estimates further downstream. However, the trend is clearly observable. Fig. 6 (right) shows the average and center velocity in the wake plotted against downstream distance. The average velocity for each downstream distance was calculated by summation of the velocity measurements in the x-z plane, as shown by Fig. 5 (left), multiplied by a contribution factor depending on the radius from the center. Thus a measurement at a larger radius from the center represents a larger annular area which leads to a larger weighting factor. Only the area with the dimensions of the rotor ($0 < r < 1$) was considered. The minimum average velocity was measured at x/R = 2 from where the velocity recovered. The center velocity reached its minimum at approximately x/R = 4 and thence stayed constant.

The turbulence measurements in Fig. 5 (right) show a similar expansion behaviour of the wake as the velocity measurements. Turbulence from the tip region shear layer propagates towards the centre of the wake which is reached at approximately x/R = 6.5. This distance marks the end of the near wake region as described by Vermeer et al. [2]. Remarkable is the passing of turbulent fluid, produced in the tower wake, through the plane observable in the lower left corner of Fig. 5 (right) between x/R = 1.5 and x/R = 3. As the tower wake is first deflected to the left more turbulent fluid is present in this region. A faster recovery due to more turbulence in the left part of the wake, as it was seen from Fig. 4 (left), could be a reason for the deformation of the wake as it was observed at x/D = 3. In addition this could explain why the area with the lowest velocity was found in the right part of the wake in Fig. 3 (right) and the wake measurements by Maeda et al. [3]. Rather than a translation of the centre to the right, the effect might be explained by a faster velocity recovery on the left part of the wake. The vorticity in the centre of the wake recovers quite fast a turbulence intensity of only 13% was measured in the centre at x/R = 2 compared to over 25% observed from the closest measurement.

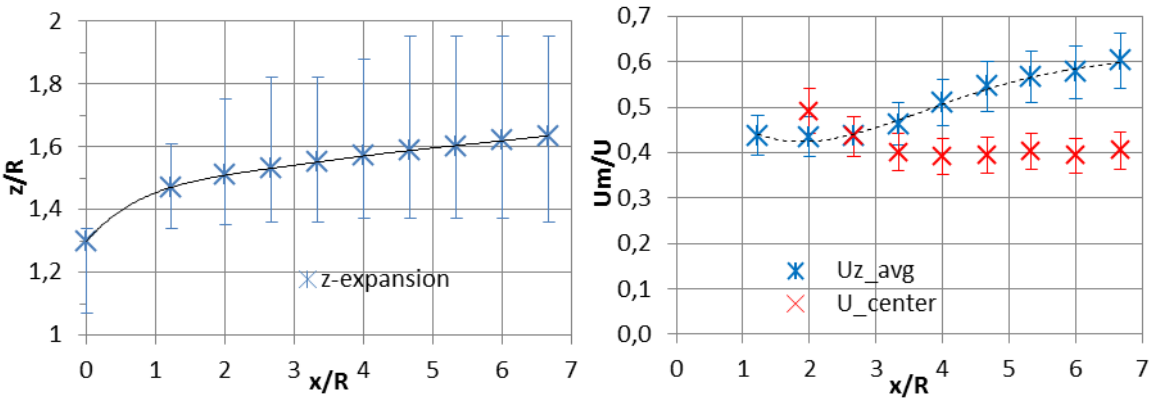

Fig. 6: Wake expansion in the z-direction for the tandem setup (left), and wake recovery of the tandem setup (right)

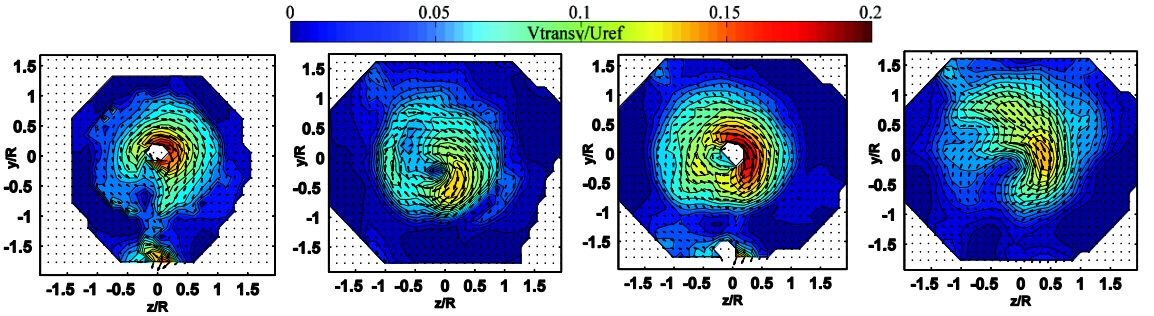

Fig. 7: Normalized velocity in the cross sectional plane normal to the x-axis at x/D=0.6 (left) and x/D=3 (second from the left) downstream of the single turbine; at x/D=0.6 (third from the left) and x/D=3 (right) downstream of the tandem setup.

3.4 Wake rotation

Fig. 7 shows the transversal velocity in the plane for the single turbine wake at x/D = 0.6 and x/D = 3 and for the tandem case at x/D = 0.6 and x/D = 3, respectively. The wake was observed to rotate faster close to the center. From the near wake measurements the tower shadow is observable for both cases. The center of rotation agreed with the rotational axis of the turbine. For the far wake the center of rotation was found to be located slightly downward and leftward of the rotational axis. This movement of the centre was thought to be a result of the presence of the tower. Measurements performed by Blomhoff [8] showed a symmetric wake as an identical fake tower was mounted on top of the turbine.

In comparison with the near wake, the far wake showed a considerably reduced and irregular velocity distribution for single and tandem wake. The tandem wake was found to rotate slightly faster than the single turbine wake and the rotating area was broader. The highest velocities, $V_{transv}/U_{\infty} \approx 0.2$ in the near wakes, were unexpectedly high. The inner wake, close to the center of rotation, was found to rotate faster than the outer wake region. This cannot be generalized. Medici [10] found the fastest rotational velocity in the tip region. Variations dependent on the design of the blades are expected.

An expression for the strength of the rotation of the wake is the swirl angle.

$$\tan\gamma = U_{\tan}/U_x \tag{1}$$

This was calculated for our measurements but strongly varies with the position as the transversal velocities in **Fig. 7** do. Therefore, it is not appropriate to give a single swirl angle for the wake. For the wake behind the single turbine swirl angles in the range from 4 to 16 ° and 3 to 11° were found at x/D = 0.6 and x/D = 3, respectively. For the wake behind the tandem setup swirl angles in the range from 5 to 23 ° and 3 to 21° were found at x/D = 0.6 and x/D = 3, respectively. Ainslie [4] mentions swirl angles less than 10° which cannot be confirmed by our measurements. Alfredsson et al. [19] reports angles of 30° at 1/3 of the wake radius and 10° at the blade tip radius. These angles are in better accordance with our results and point to a stronger rotation close to the center as mentioned before.

4. Conclusion

The measured rotor wake showed good agreement with wake theory. A highly turbulent transition zone, surrounding a relative uniform wake area was observed. The centre of the wake was characterized by stronger rotational velocities. The expansion and recovery of the wake was measured and deemed in

accordance with wake theory. In addition a tower wake, often not covered by wake theory, was measured, characterized by the highest turbulence intensity and velocity deficit. This tower wake was found to be deflected when it interacts with the rotating fluid of the rotor wake. In the far wake the tower wake was not observable anymore but was expected to cause a deformation of the wake, movement of the rotational centre and unevenly distributed turbulence maxima.

The wake of a wind turbine operating in the wake of an upstream turbine was characterized by lower velocities, higher average turbulence intensity and a slightly higher rotational speed compared to the wake of an undisturbed turbine. The higher turbulence intensity increased the mixing of the fluid and thus the recovery rate of the wake. The tower wake was less distinct in the wake of the second turbine. The overall expansion of the second turbine was larger due to the superposition with the upstream wake.

The towers of the model turbines were oversized in comparison with the dimensions of a real wind turbine. Therefore the influence of the tower is expected to be smaller for a real turbine. For wind farms the downstream turbines can experience higher loads due to an asymmetric distribution and increased values of turbulence in the upstream wake. The second row turbines in particular will be affected by the non-symmetries. An influence on the performance due to an additional velocity deficit caused by the tower is not expected. However, when the rotor wake merges with the lower tower wake and the wake expands more at the bottom part this will intensify the effect of the non-uniform horizontal velocity profile originally due to the atmospheric boundary layer.

5. References

1. Sanderse, B., *Aerodynamics of wind turbine wakes*, 2009, ECN Wind Energy.
2. Vermeer, L.J., J.N. Sørensen, and A. Crespo, *Wind turbine wake aerodynamics.* Progress in Aerospace Sciences, 2003. 39: p. 467-510.
3. Maeda, T., et al., *Wind Tunnel Study of the Interaction between Two Horizontal Axis Wind Turbines.* Wind Engineering, 2004. 28(2): p. 197-212.
4. Ainslie, J.F., *Calculating the flowfield in the wake of wind turbines.* Journal of Wind Engineering and Industrial Aerodynamics, 1988. 27: p. 213-224.
5. Talmon, A.M., *Data Report: The Wake of a Horizontal-axis Wind Turbine Model; Measurements in Uniform Approach Flow and in a Simulated Atmospheric Boundary Layer*. 1985: TNO Devision of Technology for Society.
6. Bartl, J., F. Pierella, and L. Sætran, *Wake measurements behind an array of two model wind turbines.* Energy Procedia, 2012. 24: p. 305-312.
7. Nygard, Ø.V., *Wake behind a horizontal-axis wind turbine*, in *Department of Energy and Process Engineering*2011, Norwegian University of Science and Technology: Trondheim.
8. Blomhoff, H., *An experimental investigation of wind turbine wakes*, in *Department of Energy and Process Engineering*2012, Norwegian University of Science and Technology: Trondheim.
9. Smith, D. and G.J. Taylor. *Further analysis of turbine wake development and interaction data*. in *13th BWEA Wind Energy Conference*. 1991. Swansea.
10. Medici, D., *Experimental Studies of Wind Turbine Wakes - Power Optimisation and Meandering*, in *Mechanics - Royal Institute of Technology*2005, KTH: Stockholm.
11. Adaramola, M.S. and P.-Å. Krogstad, *Experimental investigation of wake effects on wind turbine performance.* Renewable Energy, 2011. 36: p. 2078-2086.
12. Krogstad, P.-Å. and M.S. Adaramola, *Performance and near wake measurements of a model horizontal axis wind turbine.* Wind Energy, 2011. 15(5): p. 743-756.

13. Krogstad, P.-Å. and P.E. Eriksen, *"Blind test" calculations of the performance and wake development.* Renewable Energy, 2013. 50: p. 325-333.
14. Pierella, F., et al., *Invitation to the 2012 "Blind Test 2" Workshop - Calculations for two wind turbines in line*, 2012, Norwegian University of Science and Technology: Trondheim.
15. Krogstad, P.-Å. and J.A. Lund, *An experimental and numerical study of the performance of a model turbine.* Wind Energy, 2011. 15(3): p. 443-457.
16. Morrison, G.L., M.T. Schobeiri, and K.R. Pappu, *Five-hole pressure probe analysis technique.* Flow Measurement and Instrumentation, 1998. 9(3): p. 153-158.
17. Sarmast, S., *Numerical study on instability and interaction of wind turbine wakes*, in *Mechanics, Stability, Transition and Control*2013, KTH: Stockholm.
18. DeVries, O., *On the theory of the horizontal-axis wind turbine.* Ann. Rev. Fluid Mech., 1983. 15: p. 77-96.
19. Alfredsson, P.H. and J.Å. Dahlberg, *Measurements of wake interaction effects on the power output from small wind turbine models*, 1981, Aeron. Inst. of Sweden: Stockholm.